Supercurrent flow through an effective double-barrier structure

Ivar Zapata and Fernando Sols
Departamento de Fisica Teórica de la Materia Condensada, C-V and Instituto de Ciencia de Materiales "Nicolás Cabrera," Universidad Autónoma de Madrid, E-28049 Madrid, Spain
(Received 28 July 1995)

Supercurrent flow is studied in a structure that in the Ginzburg-Landau regime can be described in terms of an effective double-barrier potential. In the limit of strongly reflecting barriers, the passage of Cooper pairs through such a structure may be viewed as a realization of resonant tunneling with a rigid wave function. For interbarrier distances smaller than $d_0=\pi\xi(T)$ no current-carrying solutions exist. For distances between d_0 and $2d_0$, four solutions exist. The two symmetric solutions obey a current-phase relation of $\sin(\Delta\varphi/2)$, while the two asymmetric solutions satisfy $\Delta\varphi=\pi$ for all allowed values of the current. As the distance exceeds nd_0, a group of four solutions appears, each containing $(n-1)$ soliton-type oscillations between the barriers. We prove the inexistence of a continuous crossover between the physical solutions of the nonlinear Ginzburg-Landau equation and those of the corresponding linearized Schrödinger equation. We also show that under certain conditions a repulsive δ function barrier may quantitatively describe a superconductor-normal-superconductor (SNS) structure. We conclude that the critical current of a SNSNS structure vanishes as $\sqrt{T_c'-T}$, where T_c' is lower than the bulk critical temperature.

I. INTRODUCTION

The superconducting state is characterized by the existence of long-range phase coherence in the electron system, and its characteristic nondissipative currents are associated with spatial distortions of the macroscopic phase. Superconductivity is however not the only instance of electron transport being phase coherent over distances much larger than atomic length scales. Another important example is provided by mesoscopic normal transport, which began to be investigated about 15 years ago and which quickly matured into an active branch of solid-state physics.[1] Mesoscopic transport is realized at low enough temperatures, when electrons may preserve its phase coherence over long distances and thus undergo coherent multiple scattering by impurities or boundaries. Interest in this area stimulated experimental and theoretical research on a rich variety of mesoscopic phenomena in solids,[2] each of which is associated with a specific quantum interference process. Let us consider for a moment one of the most characteristic examples: the Aharonov-Bohm (AB) effect. This is the effect by which the electronic properties of a thin ring depend periodically on the threaded magnetic flux. As a mesoscopic phenomenon, it was first observed in narrow normal cylinders[3] and later in small rings.[4] However, the AB effect in solids had already been observed in superconducting rings not long after the discovery of the Josephson effect.[5] This observation was possible without the availability of modern nanotechnology because of the existence of long-range phase coherence in superconducting rings. Phase rigidity of the superconductor collective wave function is enforced by the spontaneous breaking of gauge symmetry. In contrast, the spatial coherence of the electron field in a normal system cannot rely on the existence of a phase transition and requires low temperatures and short length scales to make itself noticed. One may adopt the simple picture that the AB effect in a superconducting ring relies on the phase coherence of the Cooper pair wave function, while its normal ring counterpart requires coherence of the single electron propagator. This consideration leads us to the question of whether, for any given electron interference phenomenon observed in a normal mesoscopic system, there may be a Cooper pair analog that could eventually be observed in a macroscopic superconductor. We have seen that there is an AB effect for single electrons as well as for Cooper pairs. In the first case, the conductance (more generally, the current-voltage characteristics) is a function of the flux with a strong periodic component.[4] In the second case, it is the critical current (more generally, the current-phase relation) that depends periodically on the flux. The question is whether other quantum interference phenomena may also display this dual nature whereby they can be realized in the propagation of single electrons or Cooper pairs. A proper comparison of the two types of dynamics requires the resolution of the equations satisfied by the corresponding effective wave functions. In the case of normal electrons, and within the noninteracting approximation, one has to look at the wave function of Fermi electrons. In the superconducting case, the attention must be turned to the order parameter $\psi(\mathbf{r})\propto\langle\hat{\psi}_\uparrow\hat{\psi}_\downarrow\rangle$, if one wishes to obtain information on the global condensate behavior.

Within the Ginzburg-Landau (GL) approximation, $\psi(\mathbf{r})$ must be an extremum of the free-energy functional

$$F=\int d\mathbf{r}\{|(\nabla-i\mathbf{A})\psi|^2-[1-V(\mathbf{r})]|\psi|^2+\lambda|\psi|^4/2\}, \quad (1)$$

where $V(\mathbf{r})$ is an effective potential and reduced units have been used.[6,7] The parameter λ is introduced here to eventually distinguish between the nonlinear GL case ($\lambda=1$) and the linear case of a Schrödinger electron with reduced energy equal to one ($\lambda=0$). Stationary solutions of Eq. (1) must satisfy the equation

$$(i\nabla+\mathbf{A})^2\psi-[1-V(\mathbf{r})]\psi+\lambda|\psi|^2\psi=0. \quad (2)$$

From the study of Eq. (2), we plan to investigate how Cooper pairs behave under an effective potential $V(\mathbf{r})$ that, in the absence of nonlinearity, is known to yield a specific quantum interference phenomenon.

Resonant tunneling (RT) is one of the best understood and perhaps simplest quantum interference phenomenona.[8] It can occur in one dimension without the requirement of a nontrivial topology. A quantum particle undergoes resonant tunneling when it has to traverse a double-barrier structure. As a consequence of multiple inner reflection, the transmission probability is very sensitive to such parameters as the electron energy or the interbarrier distance, peaking near well-defined resonances. In this paper, we choose resonant tunneling as a case study in which to analyze the possibility of a doublefold phenomenology in quantum interference processes. For simplicity, we focus on the case of a quasi-one-dimensional superconductor and assume δ-function barriers, so that $V(\mathbf{r})$ in Eq. (2) is taken to be of the form

$$V(x)=g[\,\delta(x-a)+\delta(x+a)\,]. \tag{3}$$

In the case of g large and $\lambda=0$, Eqs. (2) and (3) yield the essential phenomenology of RT for independent electrons. For this reason, we will pay special attention to the case $\lambda=1$ with $g\gg 1$, although the crossover to moderate values of g in the nonlinear case will also be analyzed.

We must specify the transport properties we wish to compute. Ideally, one would like to compare identical device properties, such as the I-V curve, which largely characterizes a normal RT diode. However, we already encounter at this stage a major difference between the two types of systems we wish to study. Unlike in the case of normal transport, the I-V characteristic is not the relevant quantity to obtain information about the Cooper pair dynamics. The application of an external bias V creates a nonequilibrium between the populations of quasiparticles coming from each side of the structure. Only very indirectly does this change in the quasiparticle population affect the properties of the condensate, and the existing effect is very sensitive to the dynamics of single quasiparticles,[9] which is very similar to that of normal electrons. In contrast, the population of Cooper pairs cannot be driven out of equilibrium, since they can only exist in a condensed state. One could at most create a difference between the chemical potentials of the condensates on each side of a structure. However, in the case of two barriers, one only expects a straightforward realization of the ac Josephson effect.

The current carried by the condensate is driven by spatial variations of the macroscopic phase. For this reason, we focus on the study of the current-phase relation for configurations $\psi(x)$ satisfying Eq. (2) with $V(x)$ given by (3). The current-phase relation is only meaningful for a superconducting structure; thus, we can hope at best to give a qualitative comparison between the two types of RT. One might still foster hopes that something resembling the scattering wave function of a single electron might still be obtained in the formal limit of $\lambda\to 0$. As we will see, however, this is not case. Because of the difference in boundary conditions, the solutions for the superconducting order parameter obtained from Eq. (2) with $\lambda=1$ and the wave functions for Schrödinger scattering states with $\lambda=0$ fall into qualitatively different classes of solutions that do not evolve continuosly into one another as $\lambda\to 0$.

The physical explanation to the major differences between the normal and superconducting versions of RT is to be found in the existence of strong correlations among Cooper pairs, which is caused by their bosonic nature and by their large mutual overlap. The picture of independent particles undergoing coherent multiple scattering, which often applies for Schrödinger electrons in the normal state, completely breaks down in the case of Cooper pairs. The notion of many independent pairs which individually experience quantum interference and collectively combine to form a macroscopic wave function would at best be adequate for a condensate formed by noninteracting molecular pairs. However, such a scenario is not known to occur in nature. One may have superfluids made of strongly interacting bosons (case of ^{4}He) or largely overlapping pairs (^{3}He), and superconductors with large (BCS) or moderately short coherence length (case of cuprate superconductors). The strong correlation in conventional superconductors manifests itself through the nonlinear term in Eq. (2). As is characteristic of broken symmetry states, the resulting wave function is rigid and does not obey a superposition principle. We will see that the stiffness of the macroscopic wave function is the primary cause of the important differences between the Cooper pair and the individual electron scenarios.

Let us now return to the AB effect. We have already noted that it can be observed both in superconducting and normal (mesoscopic) rings. Being a direct consequence of electromagnetic gauge invariance,[10] the AB effect is of a very fundamental nature. The transport properties of a thin ring must always display a periodic (although not necessarily always observable) dependence on the magnetic flux. In contrast, the sensitivity of the current to, e.g., the interbarrier distance (for a given electron energy and for a given normalization factor) in a RT structure does not stem from any fundamental symmetry. We will see that a rich dependence of the structure of the set of solutions on the interbarrier distance does certainly exist. We will also conclude however that, at large separations, an important physical quantity like the critical current becomes essentially independent of the interbarrier distance.

The search for a Cooper pair analog of resonant tunneling has led us to investigate the interesting properties of superconducting structures that can be described by a free-energy functional of the type (1). As is proved in Appendix A, under certain conditions, a quasi-one-dimensional superconductor-normal-superconductor (SNS) structure without current concentration (S and N have the same width) can be quantitatively described by a δ function in the effective GL equation. As a consequence, the model given by Eqs. (2) and (3) can yield a quantitative description of a SNSNS structure of uniform width. We have found that the set of solutions to the corresponding GL equation can display a very rich structure. The main experimental prediction is that, in a SNSNS structure, the critical current vanishes with a law $I_c(T)\sim\sqrt{T_c'-T}$, which differs markedly from the $(T_c-T)^2$ behavior of the SNS case.[11] In addition, we find $T_c'<T_c$, i.e., for a SNSNS system, there is a depression (with respect to the SNS case) of the temperature at which the critical current vanishes.

This paper is arranged as follows. After presenting the model in Sec. II, an analytical study of the solutions to the nonlinear Eq. (4) is presented in Sec. III. In Sec. IV, we prove the inexistence of a continuous crossover between the physical solutions of Eq. (2) and those of its linear version. Some experimental predictions on temperature-dependent transport properties are discussed in Sec. V. Finally, in Sec. VI, we present some concluding remarks and comment on how some of the qualitative conclusions of the present article can be extended to other interference phenomena.

II. THE MODEL

In this paper, we wish to analyze the current-carrying solutions of the nonlinear GL equation (2) with the effective potential given by (3). We may factorize the order parameter $\psi=Re^{i\varphi}$ and write $\mathbf{a}=\mathbf{A}-\nabla\varphi$ for the superfluid velocity. The gauge-invariant electric current is then written $\mathbf{j}=-R^2\mathbf{a}$. Within the assumption of a sufficiently narrow wire (width much smaller than the coherence and penetration lengths) it is safe to neglect the dependence of $\mathbf{j}$ and ψ on the transverse variables. In these conditions, our analysis reduces to the study of the solutions of the nonlinear differential equation

$$\frac{d^2R}{dx^2}+[1-g\,\delta(x-a)-g\,\delta(x+a)]R-\frac{j^2}{R^3}-\lambda R^3=0 \quad (4)$$

for arbitrary values of g (hereafter, $\lambda=1$, unless otherwise stated). In a quasi-one-dimensional superconductor, we may choose $\mathbf{A}=0$ and write for the phase

$$\varphi(x)=j\int_0^x\frac{dx'}{R^2(x')}, \quad (5)$$

where the current density j is a conserved number, the total current through a lead of cross section A being $I=jA$. For the superconducting order parameter we are interested in solutions satisfying the boundary conditions

$$\left.\begin{aligned}R&=R_\infty\\ \varphi(x)&=qx\pm\Delta\varphi/2\end{aligned}\right\}\quad \text{for } x\to\pm\infty, \quad (6)$$

R_∞ being the biggest solution (i.e., that with the lowest free energy) of the equation

$$R^6-R^4+j^2=0. \quad (7)$$

In Eq. (6), a nonzero value of $q=j/R_\infty^2$ accounts for a linear variation of the phase at infinity,[12] and the possibility of a phase offset

$$\Delta\varphi\equiv\int_{-\infty}^{\infty}[\varphi'(x)-q]dx=j\int_{-\infty}^{\infty}\left(\frac{1}{R^2(x)}-\frac{1}{R_\infty^2}\right)dx \quad (8)$$

has been introduced. As in the single-barrier case,[12] $\Delta\varphi$ will turn out to be a most convenient parameter to classify the solutions of Eqs. (4) and (6).

One may wonder whether, apart from describing the condensate analog of resonant tunneling, the double δ barrier model may quantitatively describe a specific physical system. Fortunately, the answer is yes. It is proved in Appendix A that, within the GL approximation, a δ-function effective barrier can serve as a quantitative model for a SNS structure. More specifically, we show that, if ξ_N is the coherence length of the normal metal, the effect of a normal segment of length L inserted in a superconducting wire can be rigorously modeled by a δ function of strength

$$g=\frac{L\xi(T)}{\xi_N^2}, \quad (9)$$

provided that $L\ll\xi_N\ll\xi(T)$, where $\xi(T)$ is the temperature-dependent coherence length. Since this effective δ barrier yields the correct matching properties of a realistic SNS system,[13] we may conclude with confidence that a model with a double δ-function barrier will correctly describe a SNSNS system.[14] In addition, the fact that both the barrier strength g and the effective length a are functions of temperature for a given physical structure [note that $a=d/2\xi(T)$, where d is the physical distance between the normal islands] permits us to use temperature as a convenient driving parameter to tune $g(T)$ and $a(T)$. This property has important experimental consequences that will be discussed in Sec. V.

Regarding the temperature dependence of the effective parameters, it is interesting to note that, as $T\to T_c$, one has $g(T)\to\infty$ and $a(T)\to 0$. Therefore, the Josephson limit ($g\gg 1$) can always be explored by driving T sufficiently close to T_c. In the Josephson regime, the currents are necessarily much smaller than the bulk critical current. As a consequence, the spatial variation of the phase can be safely neglected for many purposes and the phase offset can be identified with the conventional ''phase difference'' between the two superconducting terminals, $\Delta\varphi\simeq\varphi_1-\varphi_2$. In Refs. 12 and 15 it was shown that, for large g, the critical current in the presence of a δ barrier is

$$j_c^{(1)}=1/2g. \quad (10)$$

Since the bulk ($g=0$) critical current is, in these units, $j_b=0.385$, one can derive the relation

$$g=1.30(j_b/j_c^{(1)}), \quad (11)$$

valid for large g. Going beyond the δ-barrier model, one can show that the critical current for a SNS system of arbitrary normal length L is[16]

$$j_c^{(1)}=\left[\frac{2\xi(T)}{\xi_N}\sinh\left(\frac{L}{\xi_N}\right)\right]^{-1}, \quad (12)$$

provided that the resulting j_c is much smaller than j_b. One may readily note that the result (12) is consistent with Eqs. (9) and (10) in the limit $L\ll\xi_N$.

III. EXACT SOLUTIONS

A. General properties

In this section, we study the solutions of Eq. (4) satisfying the boundary conditions (6). There is a mechanical analog that helps to understand some general properties of its solutions.[17] Equation (4) may be viewed as the force equation for a classical particle of unit mass with position R at time x moving under a potential

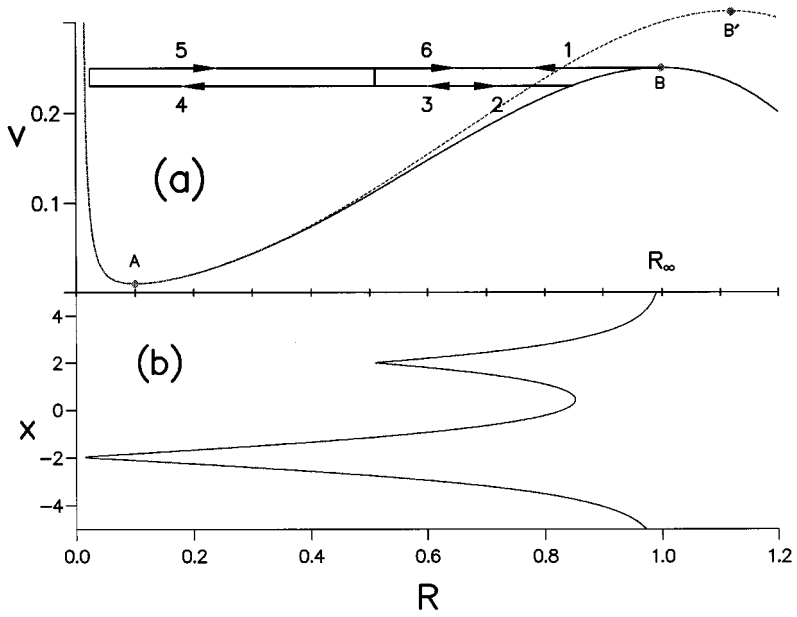

FIG. 1. (a) Potential energy $v(R)$ [see Eq. (13) in the text] for the mechanical analog of Eq. (4) with $j=0.01$, $g=2$ and $a=2$, for $\lambda=1$ (solid line) and $\lambda=0.8$ (dotted line); the straight lines depict one possible trajectory of the equivalent particle that begins and ends at point B, the numbers in the arrows indicating time-ordered flights between kicks (the distance between the two horizontal lines is exactly $\delta\varepsilon$). (b) Inverted representation of the particular solution $R(x)$ of Eq. (4) whose equivalent mechanical trajectory is that depicted in (a).

$$v(R)=-\lambda R^4/4+R^2/2+j^2/2R^2. \tag{13}$$

In the GL case ($\lambda=1$), configurations represented by points A and B of Fig. 1(a) satisfy the asymptotic condition $dR/dx=0$, with B energetically more favorable. The picture is that of a classical particle which, at remote times ($x\to-\infty$), stays in point B. At negative times, it begins to roll down and, after receiving two kicks at times $x=\pm a$, it returns asymptotically ($x\to\infty$) to point B. At each pulse, the change in the mechanical energy $\varepsilon\equiv R'^2/2+v(R)$ is determined by the matching condition

$$R'(x^+)-R'(x^-)=gR(x), \tag{14}$$

at points $x=\pm a$. Figure 1(b) shows one particular solution $R(x)$ that exactly correlates with the mechanical analogue schematically depicted in Fig. 1(a).

The energy before and after the two kicks is $\varepsilon=v(R_\infty)$. Equation (14) indicates that the effect of barriers is that of making the velocity $R'(x)$ more positive. If the system is to return to point B at $x\to\infty$, it is not difficult to see that the conditions $\delta\varepsilon_0<0$ (where $\delta\varepsilon_0$ is the change in mechanical energy at point $x=-a$) and $R'(-a^-)<0$ must be satisfied, and, for analogous reasons, $R'(a^+)>0$. These two constraints force the solutions to be of the form[18]

$$R^2(x)=Z+U\tanh^2[k(x-x_{+(-)})],\quad x>a(x<-a),$$

$$R^2(x)=e_1+(e_2-e_1)\mathrm{sn}^2\left(\sigma\sqrt{\frac{e_3-e_1}{2}}(x+a)+F_0\left|\frac{e_2-e_1}{e_3-e_1}\right.\right),\quad |x|<a, \tag{15}$$

where Z is the smallest root of $Z(Z-2)^2=8j^2$, $U\equiv 1-3Z/2$, $k\equiv\sqrt{U/2}$, and $\mathrm{sn}(x|m)$ is a Jacobi elliptic function.[18] Defining the function $y(x)\equiv R^2(x)$ and the parameters $y_0\equiv y(-a)$ and $y_0'\equiv y'(-a^-)$ (both of them functions of x_-), the matching condition (14) at $x=-a$ determines e_1,e_2,e_3 as the roots of the polynomial

$$P(s)\equiv(s-Z)(s-1+Z/2)^2+4\delta\varepsilon_0 s, \tag{16}$$

with $e_1\leqslant e_2\leqslant e_3$, and where the change in ε is

$$\delta\varepsilon_0=g(y_0'+gy_0)/2. \tag{17}$$

Finally,

$$F_0\equiv F\left(\arcsin\sqrt{\frac{y_0-e_1}{e_2-e_1}}\,\middle|\,\frac{e_2-e_1}{e_3-e_1}\right) \tag{18}$$

where $F(\varphi|m)$ is the incomplete elliptic integral of the first kind,[18] and σ in (15) is defined as

$$\sigma\equiv\mathrm{sgn}(y_0'+2gy_0). \tag{19}$$

In the limit $(y_0'+2gy_0)\to 0$, it can be shown that both values of σ in Eq. (15) lead to the same result for $R^2(x)$.

In analogy with y_0 and y_0', we define $y_1\equiv y(a)$ and $y_1'\equiv y'(a^-)$. The second kick will take us asymptotically to the value R_∞ if it causes an energy change $\delta\varepsilon_1$ such that $\delta\varepsilon_1+\delta\varepsilon_0=0$. This leads us to write the relationship

$$y_1'+gy_1+y_0'+gy_0=0 \tag{20}$$

as the global matching condition. Equation (20) determines implicitly the parameter x_- to be introduced in Eq. (15). Through the integration of Eqs. (4) and (5), each possible value of x_- uniquely determines one solution of Eq. (4) satisfying the boundary conditions (6). Thus, x_- is a parameter that completely characterizes a given physical solution. Our goal is therefore to solve numerically for all possible values of x_- satisfying Eq. (20) for a given value of j.

A quantity of interest is the critical current, which we plot in Fig. 2 as a function of the (reduced) semidistance between barriers for several values of the barrier strength. The result is given in units of the critical current for a single barrier with the same strength, $J_c(a,g)\equiv I_c(a,g)/I_c^{(1)}(g)$. For separation distances much larger than $\xi(T)$ the critical current becomes identical to that of a single barrier, regardless of the value of g. This is the limit in which the two barriers are effectively decoupled. The decoupling at long distances is

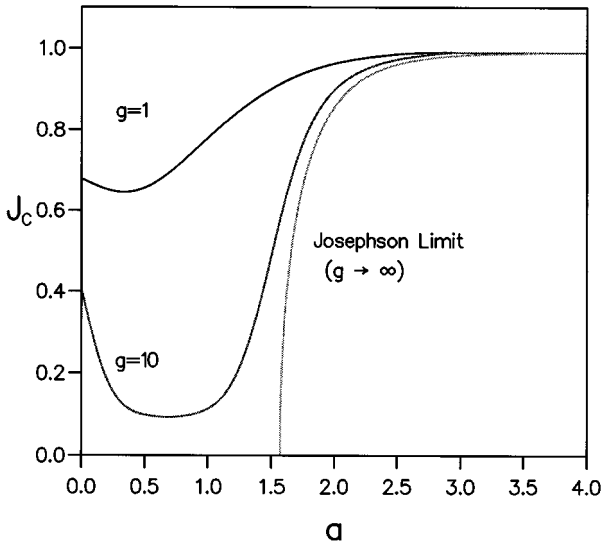

FIG. 2. Critical current as function of the semidistance between barriers for several values of the parameter g. The distance is given in units of $\xi(T)$ and the current is given in units of the critical current for a single barrier with the same g (see text).

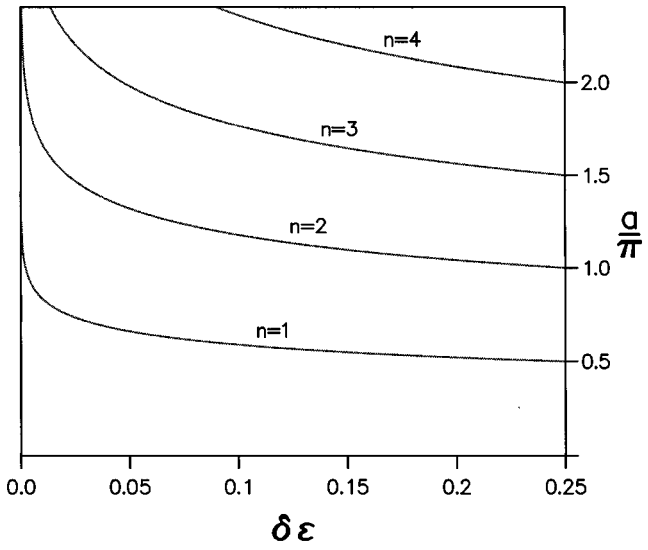

FIG. 3. Representation of the matching equation (22) in the text. The quantity $nG(\delta\varepsilon)/\pi$ is plotted for several values of the index n. A set of four solutions exists for each combination of n and $\delta\varepsilon$ that meets the requirement $nG(\delta\varepsilon)=a$, where a is the reduced semidistance between barriers.

caused by the nonlinear term in Eq. (4). In contrast, the dynamics of an electron obeying the linear Schrödinger equation is always sensitive to the presence of both barriers. We will see however that, in the nonlinear case, there are always solutions with high free energy that are sensitive to the presence of both barriers (in the sense that they cannot be viewed as simple combinations of single-barrier solutions), but these energetic solutions become increasingly irrelevant at large separations.

We observe in Fig. 2 that, for moderate values of g, there is a slight depression of the critical current with respect to the single-barrier case, if the reduced semidistance is $a \lesssim 1$ (a similar effect was noticed in Ref. 19 for the case of weak links). This effect becomes more pronounced as g gets larger. For $g=10$, the law $1/2g$ already applies approximately for the critical current of single barrier and then $J_c \simeq 1/2$ for $a=0$, as expected from a single barrier with doubled strength. Deep in the Josephson regime ($g=20$ or larger), the interval $0<a<\pi/2$ is practically depleted of solutions and the critical current is essentially zero. As will be seen later, this has noticeable experimental consequences, since the value of the reduced distance is temperature dependent. In the following two subsections, we analyze the main properties of the solutions of Eqs. (4) and (6) over the whole range of possible values of g.

B. Josephson limit ($g \to \infty$)

In the limit of large scattering strength ($g \to \infty$), the presence of a single barrier is known to yield the ideal Josephson behavior[12,15]

$$j=(1/2g)\sin(\Delta\varphi), \tag{21}$$

where the phase offset $\Delta\varphi$ can be identified with the conventional "phase difference" between the two weakly linked superconductors. For the double-barrier case, the parameter $\delta\varepsilon \equiv -\delta\varepsilon_0$ serves to characterize the continuous set of solutions in the regime of large g. For a given value of the current j, it is shown in Appendix B that $\delta\varepsilon$ takes values between 0 and $(1-J^2)/4$, where $J \equiv 2gj$ is the current in units of the critical current for a single-barrier structure. We also show in Appendix B that the matching condition (20) can be rewritten as

$$a=nG(\delta\varepsilon), \quad n=1,2,\ldots,$$

$$G(\delta\varepsilon) \equiv \left(\frac{2}{1+2\sqrt{\delta\varepsilon}}\right)^{1/2} K\left(\frac{1-2\sqrt{\delta\varepsilon}}{1+2\sqrt{\delta\varepsilon}}\right), \tag{22}$$

where $K(m) \equiv F(\pi/2|m)$ is the complete elliptic integral of the first kind.[18] For each integer n that meets the requirement (22) there are four solutions $R(x)$, all of them corresponding to the same value of $\delta\varepsilon$. The quantity $2G(\delta\varepsilon)$ is the spatial period of the solution between barriers. Thus, for each solution of Eq. (22) that we may find for a given value of n in a structure of interbarrier distance $2a$, we can always construct a solution for the structure of distance $2(a+G)$ whose index is $n+1$ and which is identical to the previous one except for the presence of an extra oscillation.

The structure of the solutions can be clearly appreciated in Fig. 3. In the Josephson limit, we see that there are no solutions for $2a<\pi$ ($J_c=0$). For $2a>\pi$ the critical current becomes nonzero and a group of four solutions appears, two symmetric and two asymmetric under the inversion $x \to -x$, the two asymmetric ones being the mirror image of each other. Their current-phase relation is shown in Fig. 4(a) for $a=1.74$. The symmetric solutions form two branches that combine to yield the curve

$$I=I_c(a,g)\sin(\Delta\varphi/2), \tag{23}$$

which is the naive expectation for two Josephson junctions in series. In contrast, the two asymmetric solutions obey the law

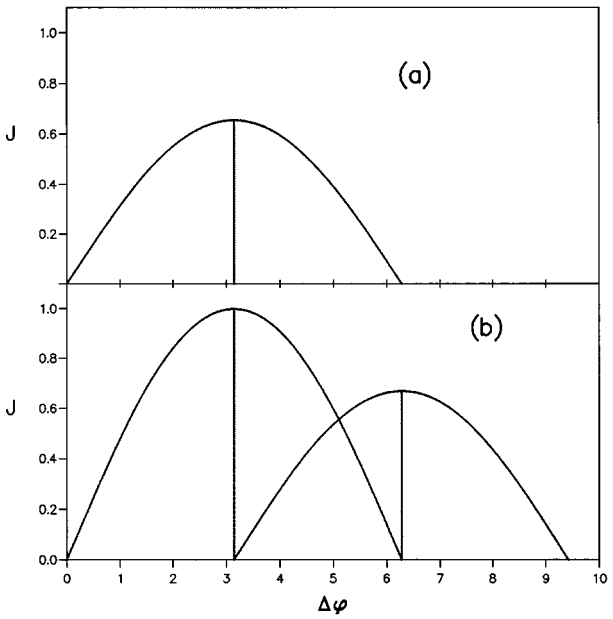

FIG. 4. Current as a function of the total phase difference for $a=1.74$ (a) and $a=3.5$ (b), in the limit of g very large. The current is given in units of the critical current for a single barrier with the same g, so that $\lim_{g\to\infty} 2gj$ is plotted.

$$\Delta\varphi=\pi, \quad \text{for all } I. \tag{24}$$

This peculiar current-phase relation can be simply understood if the two junctions are assumed to be sufficiently far apart. In this case, the central peak in $R(x)$ between the two barriers becomes a long plateau and the two barriers behave as independent. For a given current, there are two possible values of the phase, $\Delta\varphi_+$ and $\Delta\varphi_-$, satisfying Eq. (21). In the presence of the two barriers, these two phase values may combine in four different ways. In two cases, the phase difference is the same in both barriers. Then, $\Delta\varphi$ equals $2\Delta\varphi_+$ or $2\Delta\varphi_-$. This results in a $\sin(\Delta\varphi/2)$ law for the symmetric solutions. In the other two cases, a different phase change takes place in each barrier. But the total phase difference $\Delta\varphi$ is given by the sum of the two values, which is exactly

$$\Delta\varphi_+ + \Delta\varphi_- = \pi. \tag{25}$$

This explains Eq. (24) and the double vertical branch shown in Fig. 4(a). The above set of considerations makes the results (23) and (24) quite plausible, and even expected, for the case of large separations. The not so obvious result is that the same conclusions hold when the separation distance is comparable to $\xi(T)$ and the two barriers can in no way be viewed as decoupled. This result can be proved rigorously from analytical considerations (see Appendix C). The smallness of the distance between barriers makes itself noticed only through a depression of the critical current with respect to the single-barrier case, but *not* in the qualitative form of the $I(\Delta\varphi)$ curves.

As the distance grows, the maximum current of the group of four solutions saturates to the critical value for a single barrier. As indicated in Fig. 3, a new group of four solutions appears when $a>\pi$, and their current-phase relation is shown in Fig. 4(b). Comparison with Fig. 4(a) reveals two features of the $I(\Delta\varphi)$ relation: (i) for a not much larger than π, the maximum current value of the second group of solutions has not yet reached the saturation value, and (ii) all the values of $\Delta\varphi$ are shifted by π with respect to the first set of four solutions. Again, these features are easy to understand if the two barriers are assumed to be far apart. The new group of solutions resembles the first set of four, except in that a soliton (i.e., a spontaneous local depression of the gap[12]) contributing an extra phase of π has nucleated between the barriers. As the two barriers separate, the added depression of the order paramater, which may initially be viewed as the result of quantum interference oscillations, evolves into a well-defined, isolated soliton. Remarkably, the additional depression in $|\psi|$ contributes exactly π to the phase, even when the two barriers are relatively close and the depression does not act as an isolated kink but rather as an additional oscillation. It must also be noted that, since $j\neq 0$, we have $|\psi|\neq 0$ at all points.

As the separation distance is made increasingly larger, the same pattern repeats itself. Each time the distance $2a$ exceeds an integer multiple of π, a new group of four solutions appears, with a structure similar to that of the preceding set of four solutions except for an extra phase of π. As the interbarrier distance continues to increase, new sets of solutions emerge periodically, always in groups of four. For a given distance, the groups of solutions that are most sensitive to the double-barrier feature (as indicated by its not yet saturated maximum value) are those with a higher free energy resulting from a higher number of modulations in the order parameter. These very energetic solutions can be expected to be irrelevant in practice, except perhaps to account for fine details in the dynamic behavior. Therefore, it may be stated with reasonable confidence that the two barriers become effectively decoupled for practical purposes (also in regard to the dynamic behavior) when the maximum current of the second group of solutions has reached the saturation value. This happens approximately for $2a>3\pi$.

Computation of the critical current. Equation (22) (see also Fig. 3) indicates that $\delta\varepsilon$ is a unique function of a and n, so that the product in the right-hand side of Eq. (B10) must be constant within a given group of four solutions. The highest possible value of J (which is always to be found in the $n=1$ group) is obtained by imposing $\omega(1-\omega)$ to take its maximum value of 1/4. Thus we conclude that the critical current $J_c\equiv 2gj_c$ is given by the relation

$$a=\left(\frac{2}{1+\sqrt{1-J_c^2}}\right)^{1/2} K\left(\frac{1-\sqrt{1-J_c^2}}{1+\sqrt{1-J_c^2}}\right). \tag{26}$$

Equation (26) yields the curve $J_c(a)$ for the critical current in the Josephson limit, and the result has been plotted in Fig. 2.

C. Intermediate and small values of g

In Fig. 5 one can analyze the crossover between the regimes of large and small values of g for the same barrier distances we considered in the discussion of the Josephson limit (see Fig. 4). Let us comment on the case of $a=1.74$. As we depart from the limit of very large g, an extra branch appears of solutions with $\pi\leqslant\Delta\varphi\leqslant 2\pi$ and with a low criti-

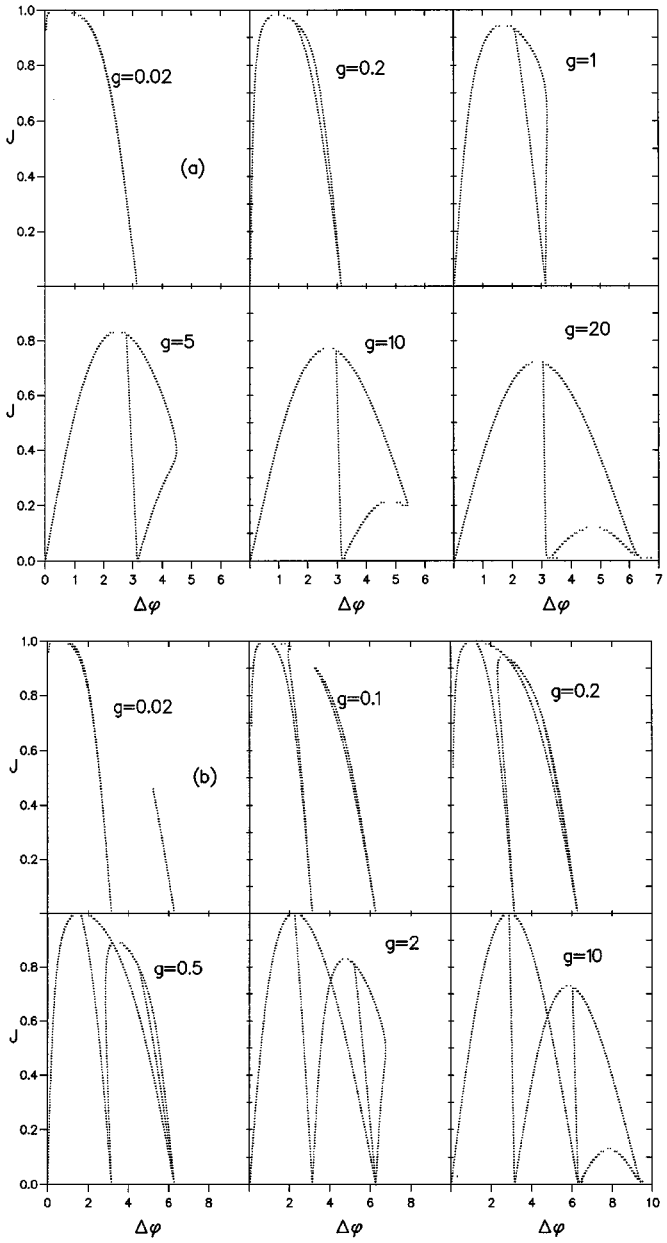

FIG. 5. Current as a function of the phase offset for several values of g in the cases $a=1.74$ (a) and $a=3.5$ (b), in the same units as in Fig. 2.

cal value [see the graph in Fig. 5(a) for $g=20$]. As g decreases further, the low current solutions with $\Delta\varphi$ near 2π disappear and the resulting branch begins to shrink until it merges (for $g\sim 0.2$) with the solutions that formed the double vertical branch in the Josephson limit. For $g\to 0$, the two sets of solutions with $\Delta\varphi\neq 0$ form a triple branch corresponding to three single solitons nucleated at points $x_0=0$ and

$$x_0=\pm\frac{1}{k}\operatorname{arctanh}\left(\frac{\sqrt{3\alpha^2-1}}{\alpha\sqrt{3-\alpha^2}}\right),\quad \alpha\equiv\tanh(ka). \qquad (27)$$

This result can be obtained analytically from the matching Eq. (20) and from the properties of the solutions (15) in the limit $g\to 0$. Meanwhile, in the same process of decreasing g, the branch of solutions with the smallest phase offset evolves towards the set of uniform solutions [those for which $R(x)=R_\infty$ and $\Delta\varphi=0$] that are characteristic of a perfect superconductor.[12]

As can be seen in Fig. 5(b), the crossover presents similar characteristics for the case where $a=3.5$. Like in the Josephson limit, the main differences for large g (with respect to previous shorter distance case) lie in the extra value of π of $\Delta\varphi$ shown by the second set of solutions and in the presence of a fourfold branch with a saturated critical current value. As g decreases, the evolution of the four solutions with higher phase offset runs similar to that of their counterparts in Fig. 5(a). New interesting features appear however for low values of g. At $g=0.5$ and 0.2 it is clear that the two groups of four solutions begin to merge into a simpler pattern of single and double solitonic solutions (with $\Delta\varphi$ tending to π and 2π as $J\to 0$, respectively). Since double soliton solutions cannot exist in the transparent case, the corresponding (fourfold) branch begins to detach from the rest of curves and to decrease its critical current until it eventually disappears. For $g\to 0$ the remaining branch is identical to its counterpart in the shorter distance case: three solutions of single solitons located in the same points as above and one uniform branch with zero phase offset. Incidentally, it can be shown that for $a\leqslant(2k)^{-1}\ln(2+\sqrt{3})$ only the soliton at $x_0=0$ survives. This is not the case however in any of the two distances considered here.

An interesting consequence of studying the crossover between large and small values of g is that, among the curves shown in Fig. 5, we can recognize similarities with current-phase relations computed for other structures that, not being exactly SNSNS, share some common features. For example, Martin-Rodero *et al.*[20] have performed a self-consistent, zero-temperature calculation of the current-phase relation in mesoscopic weak links, modeled by a tight-binding chain linked to two broad Bethe lattices that act as superconducting reservoirs. Despite of the obvious differences between the two physical models, the similarity between some of the resulting curves is striking. For instance, the current-phase relation shown for the two longest chains in Fig. 2(c) of Ref. 20 resemble some of the branches we obtain for $g=5$ and 20 in the $a=1.74$ case. It is interesting to note that the curves of Ref. 20 that look alike correspond precisely to the case of strong internal reflection at the constriction. One concludes: (i) the nonlinear term of the GL equation has an effect very similar to that of self-consistency in a zero-temperature calculation; and (ii) the essential physics rests in the nonlinear effects taking place within the finite superconducting segment and the effective scattering at its two ends, the physical details of the semi-infinite S leads being less important. Conclusion (i) is what one expects from inspecting the microscopic derivation of the GL formalism, and it has already been noted in connection with the crossover for large to small g in the single-barrier case.[12]

IV. INEXISTENCE OF A CONTINUOUS CROSSOVER BETWEEN THE LINEAR AND NONLINEAR PROBLEMS

It has already been commented in the Introduction that there are qualitative differences in the physics described by Eqs. (2)–(4) in the linear (Schrödinger) and nonlinear (GL) cases. However, one might still think that, from a mathemati-

cal point of view, there could be a continuity (as a function of λ) between the order-parameter configurations satisfying the GL equation ($\lambda=1$) and the scattering wave function for a Schrödinger electron in the presence of potential (3) with $\lambda=0$ and unit energy. Again, it is useful to consider the mechanical analog represented in Fig. 1. The wave function of a retarded scattering state is of the type $\psi\sim e^{ikx}+re^{-ikx}$, for $x\leqslant -a$, if the electron is coming from the left, so that the amplitude $R=|\psi|$ displays oscillations in the left asympotic region. The mechanical picture to introduce in Fig. 1 would be that of a particle which at remote times $x\to-\infty$ is oscillating between two return points with energy $\varepsilon<v(R_\infty)$, receives two sudden pulses at times $x=\pm a$, and ends asymptotically in one of the stationary points (this corresponds to the uniform amplitude solution $\psi\sim te^{ikx}$ to be found in the $x>a$ region). Thus we see that a major difference between the two cases lies in the asympotic behavior of $R(x)$, which is always uniform for the superconducting order parameter while it may oscillate for a Schrödinger electron. The only remaining possibility to find a common mathematical wave function must be looked for in that combination of parameters which yields a transmission unity for the electron linear wave, since in this case R would be uniform on both sides of the structure. The equivalent mechanical particle would start from a stationary point to which it would return at late times. The problem is that, for an electron satisfying the linear Schrödinger equation, that stationary point has to be A (see Fig. 1), and not B, as is the case for the GL order parameter. Although a rigorous demonstration of this statement is possible, it suffices to note that, as $\lambda\to0$, the potential maximum at B moves toward infinite values of v and R (see B' in Fig. 1 for $\lambda=0.8$), effectively disappearing from the picture when $\lambda=0$. Thus the only stationary point that is available in the linear case to describe purely transmitted waves is precisely point A, qualitatively different from B even in the limit $\lambda\to0$. We conclude that, as the nonlinear term in Eq. (4) is made to vanish ($\lambda\to0$), there does not exist a continuous crossover between the physical solutions of the nonlinear Ginzburg-Landau equation and those of the linear Schrödinger equation.

V. EXPERIMENTAL PREDICTIONS

The proximity between barriers is most noticeable when the low-energy solutions are sensitive to it. Of course, the most dramatic effects can be seen for $2a<\pi$, when no solutions exist at all in the large g limit. This has interesting experimental consequences. We must first remember that a is the reduced semidistance in units of $\xi(T)$, i.e., $a(T)=d/2\xi(T)$. This means that, for a given structure with a fixed physical distance d, the reduced distance $2a$ can be made arbitrarily small by driving the temperature sufficiently close to T_c, since then $\xi(T)=\xi_0'(1-T/T_c)^{-1/2}\to\infty$ (for a clean superconductor, $\xi_0'=0.74\xi_0$, while for a dirty superconductor $\xi_0'=0.85\sqrt{l\xi_0}$, l and ξ_0 being the mean free path and the zero-temperature coherence length, respectively[21]). If the double-barrier structure is formed by two normal segments, we know from the analysis in Sec. III that $g(T)$ scales towards the Josephson limit. Therefore, there is a temperature $T_c'<T_c$ above which $d<\pi\xi(T)$. Since, at the same time, $g(T)$ is very large, this has the consequence that no current-carrying superconducting solutions are allowed in the temperature interval $T_c'<T<T_c$. The result is that, for a SNSNS structure, there is a depression (with respect to the SNS case) in the critical temperature above which the critical current becomes zero.

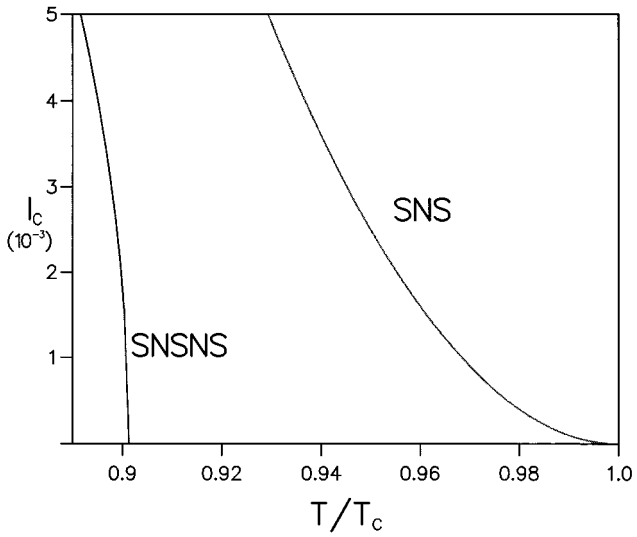

FIG. 6. Temperature dependence of the critical current in the vicinity of the critical temperature, for SNS and SNSNS structures without current concentration. $d/\xi_0'=10$ has been taken, and units are such that the prefactor of $(1-T/T_c)^2$ in Eq. (31) equals unity.

In Fig. 6, the critical current is plotted as a function of temperature for both a SNS and a SNSNS structure. The main feature of the resulting $I_c(T)$, namely, the law with which it vanishes, is amenable to an analytical treatment. In Sec. III, we derived Eq. (26), which determines $J_c(T)$ for a given value of $a(T)$. Since we are interested in finding out how the critical current vanishes, we may expand the right-hand side of Eq. (26) for small values of $J_c(T)$ and obtain

$$a(T)\equiv\frac{d}{2\xi_0'}\sqrt{\frac{T_c-T}{T_c}}\simeq\frac{\pi}{2}\left(1+\frac{3}{16}J_c^2(T)\right). \tag{28}$$

The temperature T_c' for which $J_c(T_c')=0$ is $T_c'=T_c-\Delta T_c$, with

$$\Delta T_c=\left(\frac{\pi\xi_0'}{d}\right)^2 T_c. \tag{29}$$

Equation (29) is actually an upper bound to the value of T_c-T_c', and it tends to the exact value when the condition $g(T_c')\gg1$ is consistently satisfied.

After some simple algebra, we get for the critical current (in real units):

$$I_c(T)=I_c^{(1)}(T_c')\left(\frac{8}{3\pi^2}\right)^{1/2}\left(\frac{d}{\xi_0'}\right)\left(\frac{T_c'-T}{T_c}\right)^{1/2},\quad T\to T_c', \tag{30}$$

where

$$I_c^{(1)}(T)=\frac{A}{g(T)}\left(\frac{e\hbar}{m}\right)\frac{\psi_\infty^2(T)}{\xi(T)}=\frac{A}{L}\left(\frac{\hbar c^2}{16\pi e}\right)\left(\frac{\xi_N}{\kappa\xi'^2_0}\right)^2\frac{(T_c-T)^2}{T_c^2} \tag{31}$$

is the critical current of a SNS structure at temperature T, A being the cross area of the junction and $\kappa \equiv \lambda(T)/\xi(T)$ is the Ginzburg-Landau parameter of the superconductor. The square-root behavior of $I_c(T)$ for a SNSNS structure contrasts markedly with the $(T_c - T)^2$ law of the SNS case.[11]

Simple estimates suggest that the predicted depression in the critical temperature should be measurable. For example, for a SNSNS structure made with superconducting Al ($T_c = 1.19$ K and $\xi_0 = 1.6$ μm) with $d = 10\xi_0$ (which falls within the validity of GL regime) one would obtain a decrease of $\Delta T_c \sim 0.05$ K. On the other hand, it is interesting to note that, if the condition $d \gg \xi_0$ is satisfied, there is a range of temperatures sufficiently far below T_c for which $d \gg \xi(T)$ and, thus, $I_c(T) \simeq I_c^{(1)}(T)$.

The sensitivity of the effective g to temperature can be exploited in other interesting ways. For example, by varying the temperature, one may drive a given SNS or SNSNS structure from the large to the small g regime. Consider a SNS structure made in a narrow wire of finite length at whose extremes we apply an external voltage. N is a normal metal with critical temperature $T_c < T_c$. When T gets close to T_c, $g(T)$ becomes large, and so does $\xi(T)$. Both facts contribute to yield an ideal Josephson behavior [a large value of $\xi(T)$ makes the length of the wire effectively shorter, thus facilitating the adiabatic response characteristic of the ac Josephson effect[12]]. As an external voltage is applied, the current oscillates very rapidly and one observes a zero time average, $I_{\rm av} = 0$. As the temperature is lowered below T_c, the structure becomes of the type SSS with an effective $g \lesssim 1$ (we may choose S to be not very different from S). The situation is then close to that of a uniform superconductor and the system cannot respond adiabatically to the externally applied bias.[12,17,22] Some type of resistive behavior has to be displayed, with the result that $I_{\rm av} \neq 0$. The net effect is that, by lowering the temperature, it is possible to drive a given SNS structure from adiabatic to resistive response.

VI. CONCLUSIONS

We have studied superconducting flow in structures which, in the Ginzburg-Landau regime, can be described by a double-barrier effective potential. We have found that the critical current is depressed with respect to the single-barrier case. In the limit of strongly reflecting barriers, I_c can become effectively zero for interbarrier distances $d < d_0 \equiv \pi\xi(T)$. As d exceeds d_0, four solutions (two symmetric and two asymmetric) appear, as might be expected for two Josephson links in series. As d grows even larger, new solutions appear, always in groups of four. The supression of I_c for short distances has practical consequences, since $d_0(T) \to \infty$ as $T \to T_c$, and the condition $d \leq d_0$ is always reached by any device if T is sufficiently close to T_c. Thanks to this analysis, we have found that the critical current of a symmetric SNSNS structure is lower than that of a SNS structure with an equivalent N segment. More important, the law with which $I_c(T)$ vanishes is qualitatively different in each case (see Fig. 6): $I_c(T)$ decays as $\sqrt{T_c' - T}$ in a SNSNS structure, as opposed to the $(T_c - T)^2$ behavior of the SNS case, with the inequality $T_c' < T_c$ being always satisfied.

We have also shown that, because of the different boundary conditions, the solutions of the GL equation cannot evolve continuously towards the scattering solutions of the linear Schrödinger equation as the nonlinear term is formally made to vanish.

We close this article by returning to the question that initially motivated it, namely, the possibility of finding a macroscopic quantum analog of a specific interference process such as the resonant tunneling of Schrödinger electrons. It was already commented in the Introduction that, given the important differences between the relevant transport properties of the physical systems involved, the analogy would at best be qualitative. We have learned that a basic fact such as the dependence of transport behavior on the interbarrier distance—all other parameters being equal—effectively disappears in a superconducting structure with $d \gg \pi\xi(T)$ (see Fig. 2). Since $\xi(T)$ is the length scale needed for the nonlinear term in Eq. (2) to make itself noticed, we may adopt the view that the nonlinear term in the GL equation acts as a dephasing term that damps any interference effect requiring modulation of the wave-function amplitude R (as would be caused, i.e., by the interference of waves traveling in different directions). This picture allows us to extrapolate our conclusion on the inequivalence of macroscopic and microscopic resonant tunneling to other interference phenomena. Consider, for instance, weak localization. If one considers a superconducting structure which, in the GL regime, is described by Eq. (2) with a weakly disordered effective potential $V(\mathbf{r})$, could we expect that quantum interference might cause a reduction of, i.e., the critical current? From the analysis presented here, the answer seems to be no, at least when the distance between ''impurities'' is much larger than $\xi(T)$: the nonlinear term would damp interference effects to the point of making each impurity act as isolated. In particular, one should not expect to observe the macroscopic equivalent of Anderson localization. A similar conclusion holds, in principle, for other mesoscopic phenomena based on geometry-induced quantum interference such as the modulation of current by a tuning stub:[23] one should not expect any type of interference effect associated to the collective wave function in a superconductor enclosed in a specific (topologically trivial) geometry, as long as the relevant length scales are of order $d \gg \xi(T)$. As indicated in the Introduction, real analogs are to be found only for those ''interference'' phenomena based on fundamental symmetries such as gauge invariance, which gives rise to the Aharonov-Bohm effect. A qualitative conclusion is that care must be taken when developing physical intuitions based on the idea that the superconducting order parameter plays the role of a macroscopic quantum wave function.

ACKNOWLEDGMENTS

We wish to thank Jaime Ferrer for valuable discussions. This work has been supported by CICyT, Project No. MAT91-0905, by DGICyT, Project No. PB93-1248, and by the Human and Capital Mobility Programme of the EC. One of us (I.Z.) gratefully acknowledges the support from the Comunidad Autónoma de Madrid. Support from the Institute for Scientific Interchange (Torino, Italy) is also acknowledged.

APPENDIX A: DEDUCTION OF THE δ BARRIER MODEL FOR A SNS STRUCTURE

Suppose we are given a quasi-one-dimensional SNS structure. Let the normal metal occupy the region $[-L/2,L/2]$. $T_c^{(N)}$ and $T_c^{(S)}$ are the critical temperatures of N and S, respectively. We have $T_c^{(N)}<T<T_c^{(S)}$ and assume $T_c^{(S)}-T_c^{(N)}\ll T_c^{(N)}$. Following Refs. 11 and 24, we assume that both N and S have the same order parameter to gap ratio, ψ/Δ, as well as the same quasiparticle mass. It can be proved[24] that, in these conditions, the Ginzburg-Landau equations are valid for all x, and that the matching conditions are determined by the continuity of ψ and its first derivative at $x=\pm L/2$. Thus one has

$$-\frac{\hbar^2}{2m}\frac{d^2R}{dx^2}+\alpha_S R+\beta_S R^3+\frac{mj^2}{8e^2R^3}=0 \quad |x|>L/2, \tag{A1}$$

$$-\frac{\hbar^2}{2m}\frac{d^2R}{dx^2}+\alpha_N R+\beta_N R^3+\frac{mj^2}{8e^2R^3}=0 \quad |x|<L/2, \tag{A2}$$

where $R(x)=|\psi(x)|$ and α_N,β_N (α_S,β_S) refer to the Ginzburg-Landau parameters of the normal (superconducting) metal, all of which depend on temperature.

As T approaches $T_c^{(S)}$, we can neglect the term $\beta_N R^3$ in Eq. (A2) and the remaining parameters of the normal metal can be replaced by their fixed values at $T_c^{(S)}$. Shifting to reduced units of the superconductor[7] we write

$$-\frac{d^2R}{dx^2}-R+R^3+\frac{j^2}{R^3}=0 \quad |x|>l/2, \tag{A3}$$

$$-\frac{d^2R}{dx^2}+\theta R+\frac{j^2}{R^3}=0 \quad |x|<l/2, \tag{A4}$$

where $l\equiv L/\xi(T)$. This model is identical to that considered by Jacobson[16] with

$$\theta\equiv\frac{\xi^2(T)}{\xi_N^2}\gg 1. \tag{A5}$$

If $\theta\gg j_c^2/R^4$, the integration of (A4) along the normal segment yields

$$R'(l/2)-R'(-l/2)\simeq l\theta R, \tag{A6}$$

where $\sqrt{\theta}l=L/\xi_N\ll 1$ has been assumed, so that $R(x)$ can be approximated as constant within the integral. In these conditions, the effect of the normal metal can be exactly mimicked by a δ barrier located at $x=0$ with a strength

$$g\equiv l\theta=\frac{\xi(T)L}{\xi_N^2}, \tag{A7}$$

as we wished to prove.

APPENDIX B: MATCHING IN THE JOSEPHSON LIMIT

If, from the parameters intervening in Eq. (15), we define

$$z\equiv\tanh[k(a+x_-)], \tag{B1}$$

it is not difficult to see that y_0 and y_0' defined in the text are given by

$$y_0=Z+Uz^2, \tag{B2}$$

$$y_0'=\sqrt{2U^3}(z^3-z). \tag{B3}$$

So, the condition $y_0'\leqslant 0$ implies $0\leqslant z\leqslant 1$. Equation (17) for $\delta\varepsilon_0$ can then be rewritten as

$$\delta\varepsilon_0(z)=\frac{g}{2}[\sqrt{2U^3}(z^3-z)+g(Z+Uz^2)]. \tag{B4}$$

The additional requirement $\delta\varepsilon_0<0$ implies that z is further restricted to the range $z_{\min}<z<z_{\max}$, where $z_{\min},z_{\max}$ are the roots of $\delta\varepsilon_0(z)$ lying between 0 and 1. We define ω as

$$z\equiv z_{\min}+\omega(z_{\max}-z_{\min}), \tag{B5}$$

so that, obviously, $0<\omega<1$.

In the Josephson limit ($g\to\infty$) it is easy to see that $Z\simeq J^2/2g^2$ ($J\equiv 2gj$) and $U\simeq 1$. Since, in the same limit, the only surviving finite root of $\delta\varepsilon_0(z)$ is $z=0$, we can neglect z^3 in front of z in Eq. (B4). Then $z_{\min}$ and $z_{\max}$ can be easily calculated as the roots of

$$-\sqrt{2}z+\frac{J^2}{2g}+gz^2=0. \tag{B6}$$

To leading order in $1/g$, we get

$$z_{\max,\min}=\frac{1}{g\sqrt{2}}(1\pm\sqrt{1-J^2}) \tag{B7}$$

and, from (B5),

$$z=\frac{1+(2\omega-1)\sqrt{1-J^2}}{g\sqrt{2}}+o\left(\frac{1}{g}\right), \tag{B8}$$

where $o(1/g^n)$ stands for any expression such that $\lim_{g\to\infty}g^n o(1/g^n)=0$. From Eq. (B4), we obtain, also to leading order,

$$\delta\varepsilon_0(z)=\frac{g}{2}\left(\sqrt{2}z+\frac{J^2}{2g}+gz^2\right), \tag{B9}$$

which can be easily shown to lead to

$$\delta\varepsilon\equiv-\delta\varepsilon_0=\omega(1-\omega)(1-J^2). \tag{B10}$$

For the other quantities in Eq. (15), we obtain

$$e_1=\frac{J^2}{2(1-4\delta\varepsilon)}\frac{1}{g^2}+o\left(\frac{1}{g^2}\right),$$

$$e_2=1-2\sqrt{\delta\varepsilon}+o(1),$$

$$e_3=1+2\sqrt{\delta\varepsilon}+o(1). \tag{B11}$$

The quantities β, Ω_0, Ω_1, and m are defined as

$$F_0\equiv\frac{\beta}{g}+o\left(\frac{1}{g}\right), \tag{B12}$$

$$2a\left(\frac{e_3-e_1}{2}\right)^{1/2}\equiv\Omega_0+\frac{\Omega_1}{g}+o\left(\frac{1}{g}\right), \tag{B13}$$

$$m\equiv\frac{e_2-e_1}{e_3-e_1}=\frac{1-2\sqrt{\delta\varepsilon}}{1+2\sqrt{\delta\varepsilon}}+o(1). \tag{B14}$$

In this limit, the parameter σ of Eq. (15) becomes $+1$. The global matching equation (20) can be rewritten as

$$y'(-a^+)+y'(a^-)=g[y(-a)-y(a)]. \tag{B15}$$

Solving this equation order by order in $1/g$, we get

$$\mathrm{sn}^2(\Omega_0|m)=0, \tag{B16}$$

which is equivalent to

$$\Omega_0=2nK\left(\frac{1-2\sqrt{\delta\varepsilon}}{1+2\sqrt{\delta\varepsilon}}\right),\quad n=1,2,\ldots. \tag{B17}$$

From Eqs. (B11) and (B13) we deduce

$$\Omega_0\simeq 2a\left(\frac{1+2\sqrt{\delta\varepsilon}}{2}\right)^{1/2} \tag{B18}$$

for g large, and find that Eq. (B17) leads to Eq. (22) in the text, which we wished to prove.

We also find that Ω_1 can take values $\Omega_1=-2\beta$ (for the two symmetric solutions) or $\Omega_1=-\Omega_0/a$ (for the two asymmetric ones). Solutions come in pairs because of the quadratic character of Eq. (B10). The behavior under the transformation $x\to -x$ can be deduced from the expression for the solution, which to leading order in $1/g$ takes the form

$$y_n(x)\simeq e_1+e_2\mathrm{sn}^2\left(\frac{2nK+\Omega_1/g}{2a}x+nK+\frac{2\beta+\Omega_1}{2g}\left|\frac{1-2\sqrt{\delta\varepsilon}}{1+2\sqrt{\delta\varepsilon}}\right.\right), \tag{B19}$$

where K stands for the elliptic integral in (B17).

APPENDIX C: OFFSET IN THE JOSEPHSON LIMIT

One can insert the asymptotic expressions obtained for $R^2(x)$ in the previous appendix into the second integral of Eq. (8) and make use of the identity:

$$\lim_{g\to\infty} g\int_{NK(m)+\alpha/g}^{MK(m)-\beta/g}\frac{du}{1+g^2\gamma\,\mathrm{sn}^2(u|m)} \tag{C1}$$

$$=\frac{1}{\sqrt{\gamma}}\left[\left(\frac{\pi}{2}-\arctan(\alpha\sqrt{\gamma})\right)\delta_N+\left(\frac{\pi}{2}-\arctan(\beta\sqrt{\gamma})\right)\delta_M+\pi N_e\right], \tag{C2}$$

valid for integers N,M and arbitrary positive values of α,β,γ, with $0<m<1$. In Eq. (C2), N_e is the number of even integers p satisfying $N<p<M$, and δ_N is defined as one (zero) for N even (odd). After some lengthy but straightforward algebra, one can prove that the current-phase relation for the solutions of Eq. (22) is ($J>0$)

$$J(\Delta\varphi)=\sqrt{1-4\delta\varepsilon}\left|\sin\left(\frac{(n+1)\pi-\Delta\varphi}{2}\right)\right|,$$

$$\Delta\varphi\in[(n-1)\pi,(n+1)\pi], \tag{C3}$$

for the symmetric solutions, and

$$\Delta\varphi=n\pi,\quad \text{for all } J, \tag{C4}$$

for the asymmetric solutions.

---

[1] For a review, see Y. Imry, in *Directions in Condensed Matter*, edited by G. Grinstein and E. Mazenko (World Scientific, Singapore, 1986); C.W.J. Beenakker and H. van Houten, in *Solid State Physics: Advances in Research and Applications*, edited by H. Ehrenreich and D. Turnbull (Academic, New York, 1991), Vol. 44.

[2] *Mesoscopic Phenomena in Solids*, edited by B.L. Altshuler, P.A. Lee, and R.A. Webb (North-Holland, Amsterdam, 1991).

[3] D.Yu. Sharvin and Yu.V. Sharvin, JETP Lett. **34**, 272 (1981).

[4] For a review, see S. Washburn and R.A. Webb, Adv. Phys. **35**, 375 (1986).

[5] R.C. Jaklevic, J. Lambe, A.H. Silver, and J.E. Mercereau, Phys. Rev. Lett. **12**, 159 (1964).

[6] F. Sols, J. Ferrer, and I. Zapata, Physica B **203**, 467 (1994).

[7] In these units, $\xi(T)$ is the unit of length, the order parameter ψ is measured in units of ψ_∞ (absolute value of the bulk order parameter at zero current), and $2e(\hbar/m)[\psi_\infty^2/\xi(T)]=c\sqrt{2}H_c(T)/4\pi\lambda(T)$ is the unit for current (H_c and λ are the critical magnetic field and the penetration depth, respectively).

[8] For an overview, see, for instance, *Resonant Tunneling in Semiconductors: Physics and Applications*, edited by L.L. Chang, E.E. Méndez, and C. Tejedor, (Plenum, New York, 1991).

[9] J. Sánchez-Cañizares and F. Sols, J. Phys. Condens. Matter **7**, L317 (1995).

[10] F. Bloch, Phys. Rev. B **2**, 109 (1970).

[11] A. A. Abrikosov, *Fundamentals of the Theory of Metals* (North-Holland, Amsterdam, 1988).

[12] F. Sols and J. Ferrer, Phys. Rev. B **49**, 15 913 (1994).

[13] A δ-function model to describe a SNS structure has been used by A.F. Volkov, Zh. Éksp. Teor. Fiz. **66**, 758 (1974) [Sov. Phys. JETP **39**, 366 (1974)], apparently based only on correct intuitive grounds.

[14] Equation (23) of Ref. 12 would only apply for $L\gg\xi_N$, a limit for which, unlike stated there, we have not found a rigorous justifi-

cation for the use of a δ-function model.
[15] J. Ferrer and F. Sols, Physica B **194-196**, 1751 (1994).
[16] D.A. Jacobson, Phys. Rev. **138**, A1066 (1965).
[17] J.S. Langer and V. Ambegaokar, Phys. Rev. **164**, 498 (1967).
[18] M. Abramowitz and I.A. Stegun, *Handbook of Mathematical Functions* (Wiley, New York, 1972).
[19] Y.S. Way, K.S. Hsu, and Y.H. Kao, Phys. Rev. Lett. **39**, 1684 (1977).
[20] A. Martin-Rodero, F.J. García-Vidal, and A. Levi-Yeyati, Phys. Rev. Lett. **72**, 554 (1994).
[21] M. Tinkham, *Introduction to Superconductivity* (McGraw-Hill, New York, 1975).
[22] P. M. Goldbart, Bull. Am. Phys. Soc. **36**, 540 (1991).
[23] F. Sols, M. Macucci, U. Ravaioli, and K. Hess, Appl. Phys. Lett. **54**, 350 (1989).
[24] R.O. Zaitsev, Sov. Phys. JETP **21**, 1178 (1965); **23**, 702 (1966).